Carbohydrate Polymers 116 (2015) 286–291

Contents lists available at ScienceDirect

Carbohydrate Polymers

journal homepage: www.elsevier.com/locate/carbpol

Processing of α-chitin nanofibers by dynamic high pressure homogenization: Characterization and antifungal activity against *A. niger*

Asier M. Salaberria, Susana C.M. Fernandes*, Rene Herrera Diaz, Jalel Labidi**

Biorefinery Processes Research Group, Department of Chemical and Environmental Engineering, Polytechnic School, University of the Basque Country (UPV/EHU), Pza. Europa 1, 20018 Donostia-San Sebastian, Spain

ARTICLE INFO

Article history:
Received 17 December 2013
Received in revised form 7 April 2014
Accepted 9 April 2014
Available online 21 April 2014

Keywords:
α-Chitin nanofibers
High pressure homogenization
Morphology
Antifungal activity

ABSTRACT

Chitin nano-objects become more interesting and attractive material than native chitin because of their usable form, low density, high surface area and promising mechanical properties. This work suggests a straightforward and environmentally friendly method for processing chitin nanofibers using dynamic high pressure homogenization. This technique proved to be a remarkably simple way to get α-chitin into α-chitin nanofibers from yellow lobster wastes with a uniform width (bellow 100 nm) and high aspect ratio; and may contributes to a major breakthrough in chitin applications. Moreover, the resulting α-chitin nanofibers were characterized and compared with native α-chitin in terms of chemical and crystal structure, thermal degradation and antifungal activity. The biological assays highlighted that the nano nature of chitin nanofibers plays an important role in the antifungal activity against *Aspergillus niger*.

1. Introduction

Chitin is the most abundant nitrogen-bearing compound in nature and the second most abundant biopolymer on earth after cellulose. Despite being one of the most widespread natural polysaccharide, chitin was for a long time considered as an intractable polymer because of its lack of solubility in common solvents (even in some typical cellulose solvents), which limits its processing and practical utilization (Rinaudo, 2006). However, recent studies have mainly focused on other aspects of chitin: chitin nanoparticles (Mincea, Negrulescu, & Ostafe, 2012; Zeng, He, Li, & Wang, 2012) and their applications, especially in reinforcing polymer nanocomposites (Ifuku et al., 2012; Wang et al., 2013; Zeng et al., 2012).

In nature, chitin occurs as micro/nanofibrils that form a composite together with proteins, pigments and calcium carbonate and has a structural role in the exoskeleton of crustaceans and insects (Chen, Lin, Mckittrick, & Meyers, 2008; Raabe, Sachs, & Romano, 2005). The cross-sectional width of the crystalline fibrils could range from 2.5 to 25 nm, depending on their biological origin (Revol & Marchessault, 1993).

The unique properties of chitin nanoparticles – such as their renewable and biodegradable character, extremely small size, low density, chemical stability, biological activity, and noncytotoxicity – make them excellent candidates for use in extensive range of medical applications, nanocomposite fields, water treatment, cosmetics, electronics devices, etc. (Zeng et al., 2012). For this reason, nanocrystals/whiskers and nanofibers have been obtained from crab tendons and shells, shrimp shells, lobster, squid-pen, among others, by different methods using chemical and/or mechanical treatments (Fan, Fukuzumi, Saito, & Isogai, 2012; Fan, Saito, & Isogai, 2008, 2010; Goodrich & Winter, 2007; Ifuku et al., 2009, 2010, 2011; Kadokawa, Takegawa, Minea, & Prasad, 2011; Mincea et al., 2012; Paillet & Dufresne, 2001; Qi et al., 2013; Watthanaphanit, Supaphol, Tamura, Tokura, & Rujiravanit, 2008; Zhao, Feng, & Gao, 2007) from pure chitin after removal the other exoskeleton compounds.

Chitin nanofibers have previously been processed by different methods including ultrasonic technique under neutral (Zhao et al., 2007) and acidic (Fan et al., 2008) conditions; and grinding treatment in never-dried state (Ifuku et al., 2009) and in dried state of chitin under acidic (Ifuku et al., 2010), and neutral (Ifuku et al., 2011) conditions. Despite these studies, there is still much valuable work to be done in the development of new simple and

* Corresponding author. Tel.: +34 943017163; fax: +34 943017130.
** Corresponding author. Tel.: +34 943017178; fax: +34 943017130.
E-mail addresses: susana.fernandes@ehu.es (S.C.M. Fernandes), jalel.labidi@ehu.es (J. Labidi).

http://dx.doi.org/10.1016/j.carbpol.2014.04.047
0144-8617/

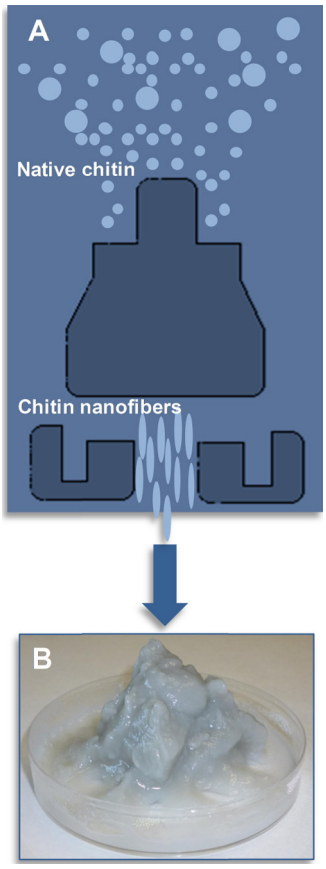

Fig. 1. Schematic diagram illustrating the straightforward way (high pressure homogenization) to isolate α-chitin nanofibers from native α-chitin flakes (this scheme is based on the GEA Niro Soavi homogenizing valves illustration of their website, 18.11.13) (A); final gel-like aqueous matter of α-chitin nanofibers after filtration (4 wt%) (B).

effective processing methods to isolate chitin nanofibers without severe degradation and practical cost.

Herein, we chose to exploit a remarkably straightforward way – dynamic high pressure homogenization – to get chitin into a usable form: nanofibers. Dynamic high pressure homogenization is based on the use of very high pressure on fluids to subdivide dispersed particles into very small sizes (order of magnitude of nanometers) (Fig. 1). This methodology provides a convenient, versatile, and environmentally friendly method for processing chitin nanofibers on a large scale which will contribute for a major breakthrough in chitin applications. On this basis, for the first time, individualized α-chitin nanofibers with diameters bellow 100 nm were processed by this simple concept. The resulting chitin nanofibers were characterized in terms of morphology, chemical and crystal structures, and thermal stability.

Chitin and its derivative chitosan have emerged as promising natural biodegradable antimicrobial and antifungal agents (Zhang, Li, & Liu, 2011). Nonetheless, thanks to the positive charge on the C-2 of the glucosamine monomer below pH 6, chitosan is more soluble and is known to present better antimicrobial activity than chitin. For this reason, the possible mechanisms discussed are mainly focused on chitosan (Kong, Chen, Xing, & Park, 2010; Krajewska, Kyzioł, & Wydro, 2013; Krajewska, Wydro, & Jańczyk, 2011; Krajewska, Wydro, & Kyzioł, 2013; Rabea, Badawy, Stevens, Smagghe, & Steurbaut, 2003; Zhang et al., 2011). Although chitin has been described as an antifungal agent, the antifungal activity of chitin nanofibers have not been evaluated previously. Here, we demonstrated that the nano nature of chitin nanofibers plays an essential role in the antifungal activity against *Aspergillus niger*.

2. Experimental

2.1. Materials

Lobster wastes (*Cervimunida johni*) in the form of flakes were kindly supplied by Antartic Seafood S.A. (Chile) and used as starting material. Anhydrous NaOH pellets, HCl (37%, w/w), acetone and ethanol were of analytical grade and purchased from Sigma–Aldrich. All reagents were used as received without further purification.

2.2. Extraction of α-chitin

Before isolating chitin nanoforms, *C. johni* lobster (known as yellow squat lobster) wastes were purified to obtain α-chitin according to conventional methods (Agulló et al., 2004). Three main steps were applied in the following sequence: (i) deproteinization – removal of proteins with NaOH (2 M) for 24 h at room temperature; (ii) demineralization – removal of minerals ($CaCO_3$) in HCl (2 M) for 3 h at room temperature (iii) decolorization – extraction of pigments and lipids using acetone followed by ethanol for 6 h under reflux. Finally, α-chitin was filtered and washed with distilled water. A sample of the resulting α-chitin was dried at 60 ± 5 °C overnight in an oven and grinded to obtain a powder for determination of yield, ^{13}C NMR measurement and antifungal activity evaluation. The yield of purified α-chitin was 15% based on the dry weight of the yellow squat lobster waste. The degree of N-acetylation of the obtained chitin was found to be 96% by ^{13}C NMR (Duarte, Ferreira, Marvão, & Rocha, 2002).

2.3. Processing of α-chitin nanofibers

α-Chitin nanofibers (CHNF) were obtained using a dynamic high pressure homogenizing (GEA Niro Soavi S.p.A, Italy). Extracted dry α-chitin was first dispersed in distilled water at 1 wt% and pretreated using an Ultra-Turrax (10,000 rpm for 5 min) followed by ultrasonic treatment for 5 min. The aim of this pre-treatment was to facilitate the passage of the dry α-chitin flakes through the homogenizing valve. The α-chitin suspension was then passed through the dynamic high pressure homogenizing with an operating pressure of 1000 bar. The number of passes of the suspension through the homogenizing valve at high pressure was forty to obtain well dispersed α-chitin nanofibers with diameters to the order of magnitude of nanometers. Finally, α-chitin nanofibers were filtered to get a final suspension of 4 wt% and were stored at 4 °C before used. A sample of the ensuing α-chitin nanofibers was dried at 60 °C ± 5 °C overnight in an oven and grinded to obtain a powder for ^{13}C NMR, ATR-FTIR, X-ray diffraction and TGA measurements and antifungal activity evaluation. The degree of N-acetylation was found to be 97% by ^{13}C NMR (Duarte et al., 2002).

2.4. Characterization

Atomic force microscopy (AFM) measurements were performed in a Dimension 3100 NanoScope IV (Veeco, USA). The images were scanned in tapping mode under ambient conditions using silicon nitride cantilevers having a tip nominal radius of 10 nm.

Attenuated total reflectance-Fourier transform infrared spectroscopy (ATR-FTIR) was used to analyze the chemical structure of chitin nanofibers. ATR-FTIR spectra of the samples were recorded on a Nicolet Nexus 670 equipped with a KRS-5 crystal of refractive index 2.4 and using an incidence angle of 45°. The spectra were taken in a transmittance mode in the wavenumber range

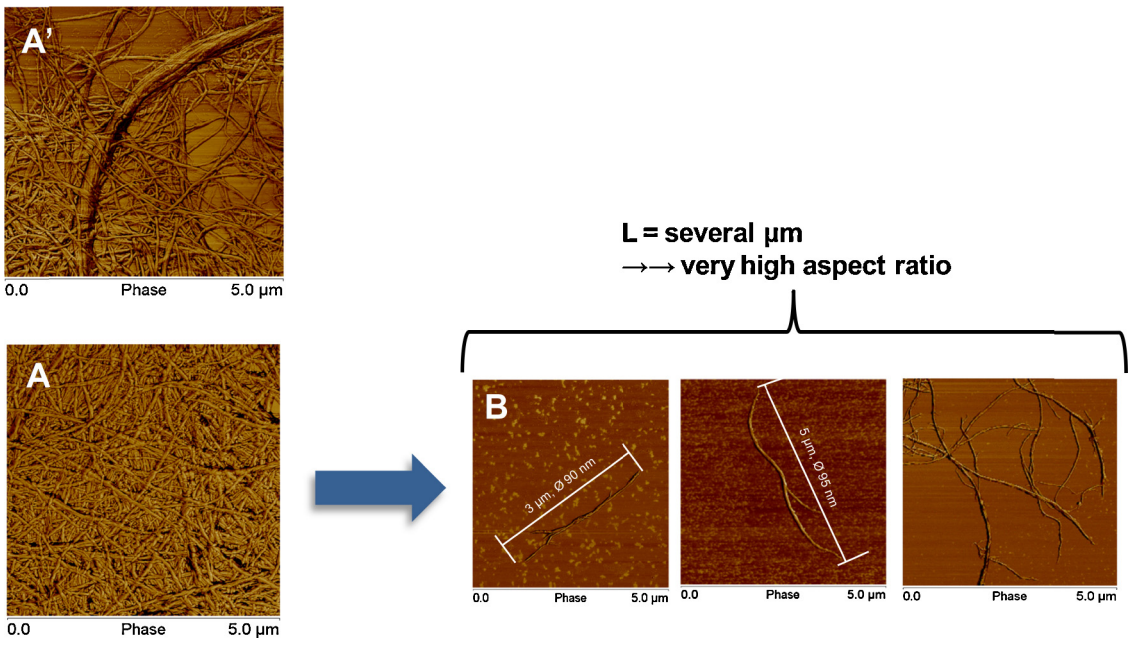

Fig. 2. AFM phase-contrast image of α-chitin nanofibers on mica after pass through the homogenizing valve: 20 times (A′), and 40 times (A); and individualized α-chitin nanofibers on mica (B). The samples were prepared using the 4 wt% aqueous suspension which was diluted to the concentration of 0.1 wt% (image A′ and A) and 0.01 wt% (image B).

of 750–4000 cm^{-1}, with resolution of 4 cm^{-1} and after 128 scan accumulations.

X-ray diffraction patterns were measured with a Philips X'pert Pro automatic diffractometer using Cu Kα radiation (operating at 40 kV and 40 mA) over the angular range of 5–40°.

The crystallinity index (C.I.) of the chitin nanofillers was calculated as follows (Focher, Beltranme, Naggi, & Torri, 1990):

$$\text{C.I.}\ (\%) = \left[\frac{I_{1\,1\,0} - I_{am}}{I_{1\,1\,0}}\right] \times 100 \quad (1)$$

where $I_{1\,1\,0}$ is the maximum intensity (arbitrary units) of the 1 1 0 crystallographic plane and I_{am} is the amorphous portion diffraction, which usually is found about 2θ = 12.5–13.5°.

Thermogravimetric analysis (TGA) assays were carried out with a TGA/SDTA 851 Mettler Toledo instrument. Samples were heated at a constant rate of 10 °C min^{-1} from room temperature to 900 °C under a nitrogen atmosphere of 20 mL min^{-1}. The thermal decomposition temperature was taken as the onset of significant (≥0.5%) weight loss, after the initial moisture loss.

2.5. Antifungal activity

In order to evaluate the antifungal activity of α-chitin nanofibers against *A. niger*, each sample was prepared in the form of pellet (13 mm in diameter and 0.4 mm in thickness) putting 50 ± 5 mg of dry α-chitin nanofibers into a cylindrical holder and pressing them using a hydraulic press. The resulting pellets were exposed to the fungus which was previously cultured in solid substrate of potato dextrose agar (PDA, Merck) and allowed to grow for 72 h at 25 ± 2 °C in sealed Petri dishes. For each experiment (three replicates), an aliquot (100 μL) of this culture was diluted in Ringer solution (100-fold), and 100 μL of the diluted suspension were aseptically inoculated on the surface of PDA agar plates containing one α-chitin nanofibers pellet. Three other replicates were done using dry native α-chitin pellets (prepared in the same manner as the α-chitin nanofibers pellets) to determine the fungal inhibition (control test). These analyze were performed following the NP 3277-1 (1987) norm. After 7 days of incubation at 25 ± 2 °C, the number of colonies was counted, and the number of colony forming units per milliliter (CFU mL^{-1}) was determined by microscopic analysis using a Neubauer chamber cell counting and lactophenol cotton blue (LPCB) to staining and observing fungi. The fungal growth inhibition (FGI) was calculated from the following relation:

$$\text{FGI}\ (\%) = \left[\frac{C_g - T_g}{C_g}\right] \times 100 \quad (2)$$

where C_g is the average concentration in the control sample set and T_g is the average concentration in the treated set (test sample), both expressed in CFU mL^{-1} (Pinto et al., 2013). The values obtained for the concentration of each sample correspond to the average of three independent experiments.

3. Results and discussion

3.1. Processing of α-chitin nanofibers

α-Chitin nanofibers were obtained from yellow squat lobster wastes (starting material) after α-chitin extraction/purification according to conventional methods (Agulló et al., 2004). Dynamic high pressure homogenization was used as a simple and environmentally friendly method to process chitin nanofibers. This method is based on the passage of the purified native α-chitin suspension (1 wt% in water) at very high pressure through an homogenizing valve with an adjustable gap (Fig. 1A), which is able to downsize chitin particles to the order of magnitude of nanometers and create a stable dispersion. The resulting material is a slightly opaque gel-like aqueous matter with a concentration of 4 wt% (Fig. 1B).

The morphology of the resulting nanoscale chitin after pass through the high-pressure homogenization is shown in Fig. 2A and B. AFM phase-contrast image of Fig. 2A shows a uniform network of α-chitin nanofibers whose cross-sectional widths are consistently between 80 and 100 nm and estimated lengths of several micrometers. Complete individualization of α-chitin nanofibers can be achieved by the present downsizing process as shown by the AFM phase-contrast images in Fig. 2B. These AFM micrographs show well-defined, distinctly individualized and long α-chitin nanofibers

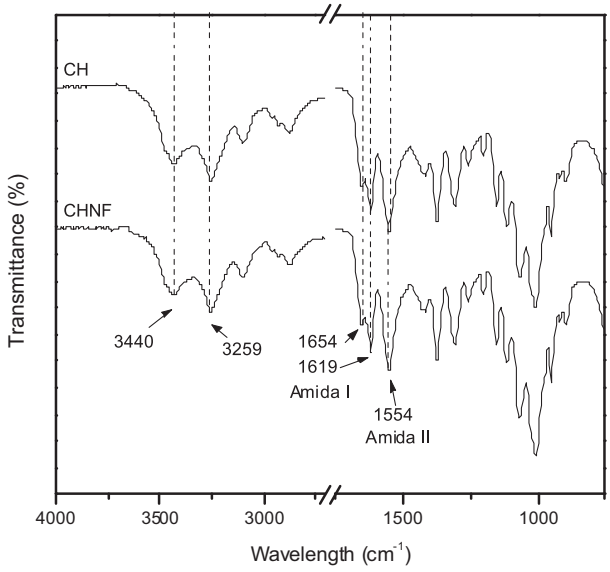

Fig. 3. ATR-FTIR spectra of native α-chitin (CH) and α-chitin nanofibers (CHNF) obtained by mechanical treatment – dynamic high pressure homogenization.

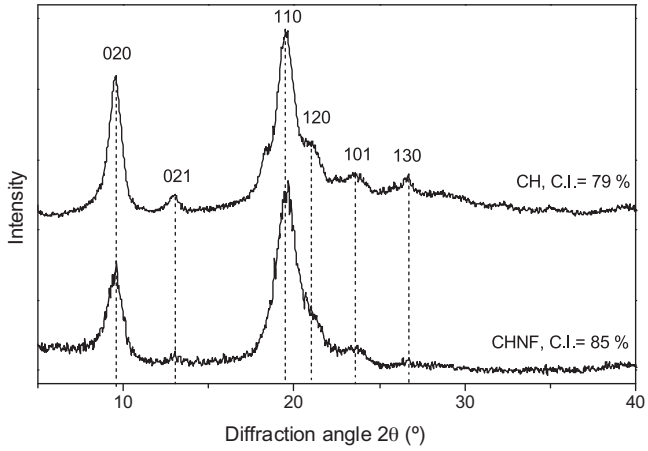

Fig. 4. XRD profile of α-chitin (CH) and α-chitin nanofibers (CHNF) and their crystallinity index (C.I.).

which present mostly 5 μm of length as well as a minority of longer lengths between 8 and 10 μm, and high aspect ratio (greater than 60).

The AFM micrograph of Fig. 2A′ corresponds to the α-chitin nanofibers after pass through the homogenizing valve twenty times. In these conditions, the sample was not completely fibrillated by the homogenizing equipment, as revealed in Fig. 2A′ by the presence of a thick fibril aggregate bundle (diameter of ~450 nm).

This work demonstrated that dynamic high pressure shear forces constitutes a novel and simple method to prepare α-chitin nanofibers with a well controlled diameter in the nanometer range (bellow 100 nm) and to maintain high aspect ratio, in contrast to chemical methods (Fan et al., 2010; Kadokawa et al., 2011; Mincea et al., 2012; Qi et al., 2013; Watthanaphanit et al., 2008).

Ifuku et al. (2011) also extracted chitin nanofibers (from black tiger prawn shell) in neutral conditions using only mechanical treatment. In this case, the disintegration was made using a grinder without any acid to obtain chitin nanofibers with diameters in the range of 10–20 nm and few microns in length. In other previous works, a dependence on chemical treatments combined with mechanical treatment was necessary to get chitin into chitin nanofibers (Fan et al., 2008; Ifuku et al., 2009, 2010; Zhao et al., 2007).

3.2. Chemical and crystal structure

ATR-FTIR spectra of α-chitin and α-chitin nanofibers are shown in Fig. 3. The two spectra are very similar presenting the characteristic absorption bands of α-chitin at 1619 cm^{-1} and 1654 cm^{-1} (amide I, singly H-bonded and doubly H-bonded, respectively), 1558 cm^{-1} (amide II), 3253 cm^{-1} (N—H stretching band) and at 3433 cm^{-1} (O—H stretching band) (Brugnerotto et al., 2001). Furthermore, no absorbing bands were observed at 1540 cm^{-1} indicating the nonexistence of residual protein in both samples (Morin & Dufresne, 2002). The presence of the chitin characteristic bands in the α-chitin nanofibers spectrum shows that the chemical structure of the α-chitin was unchanged and no N-deacetylation occurs (see data of the degree of N-acetylation in the experimental section) during the mechanical treatment.

The crystal structures of α-chitin and α-chitin nanofibers were analyzed by their X-ray diffraction patterns (Fig. 4). Mainly five crystalline reflections were observed in the 2θ range of 5–40 for both. α-Chitin nanofibers presented typical diffraction patterns of α-chitin at 9.5°, 19.5°, 21.0°, 23.5° and 26.5° indexed as 0 2 0, 1 1 0, 1 2 0, 1 0 1 and 1 3 0 planes, respectively (Feng, Liu, & Hu, 2004; Kumirska et al., 2010; Muzzarelli et al., 2007). The stronger reflections were observed at 9.5° and 21.0° and the lower reflections at higher 2θ values (e.g. 26.5° and higher) (Kumirska et al., 2010). The crystalline structure of α-chitin nanofibers remained the same after the isolation process, and the crystallinity index (C.I.) increased from 79% (CH) to 85% (CHNC).

3.3. Thermal stability

Thermogravimetric analysis (TGA) of α-chitin and α-chitin nanofibers were carried out to evaluate their thermal stability and degradation profiles (Fig. 5). Thermal degradation of α-chitin nanofibers in nitrogen atmosphere started at around 200 °C with a major degradation peak at 300 °C. Native α-chitin presented a higher thermal degradation point at 345 °C (Jang, Kong, Jeong, Lee, & Nah, 2004). Thus, the conversion of α-chitin to α-chitin nanofibers induces to some decreases in thermal stability; similar to the phenomenon reported previously (Fan et al., 2012).

The mass losses at around 100 °C of both profiles were associated with the volatilization of water.

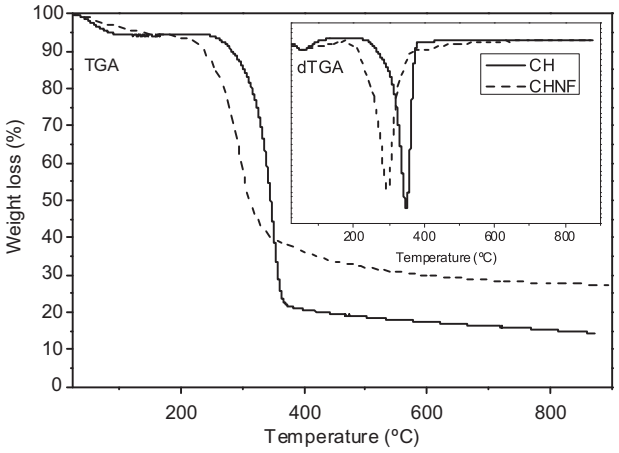

Fig. 5. Thermogravimetric curves (TGA) and derivative curves (dTGA) of native α-chitin (CH) and α-chitin nanofibers (CHNF).

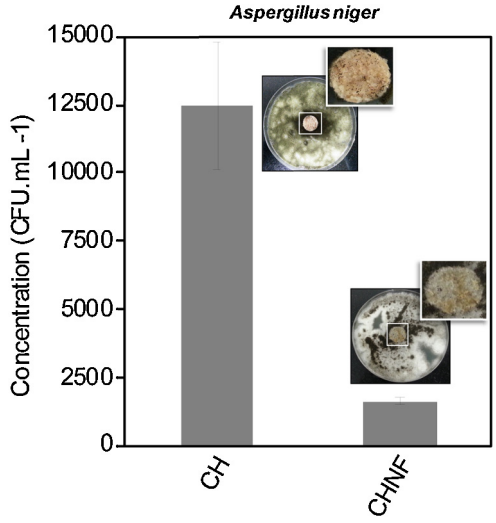

Fig. 6. CFU mL^{-1} counts and digital photographs of PDA plates containing *A. niger* in contact with native α-chitin (CH, control sample) and α-chitin nanofibers (CHNF) pellets after 7 days of incubation.

3.4. Antifungal activity

As a first step to investigate the antifungal activity of α-chitin nanofibers, *A. niger*, a common species of the genus *Aspergillus* recognized as the most contributor agent in food contamination (Plascencia-Jatomea, Viniegra, Olayo, Castillo-Ortega, & Shirai, 2003), was inoculated in PDA plates containing α-chitin nanofibers.

Fig. 6 shows the CFU mL^{-1} counts and digital photographs of the viable colonies of *A. niger* on PDA plates, after 7 days of incubation at 25 ± 2 °C, of native α-chitin (CH, control sample) and α-chitin nanofibers (CHNF). The colony forming units (CFU mL^{-1}) of both samples and the fungal growth inhibition (FGI %) of α-chitin nanofibers are listed in Table 1.

Interestingly, the results revealed that α-chitin nanofibers have superior antifungal activity on *A. niger* growth than native α-chitin (Fig. 6). Thus, there is a strong correlation between the growth inhibition of *A. niger* and the nano nature of the chitin nanofibers, i.e. small and compact size and high surface area/charge.

Although, the exact mechanism of the antimicrobial action of chitin, chitosan, and their derivatives is still limited and unclear, several mechanisms have been proposed (Kong et al., 2010; Krajewska et al., 2011; Krajewska, Kyzioł, et al., 2013; Krajewska, Wydro, et al., 2013; Rabea et al., 2003; Zhang et al., 2011). The mode of antimicrobial action of chitin and chitosan has been associated to mechanisms that include their penetration in the cell wall of fungi and bind to its DNA, inhibiting the synthesis of mRNA and, thus, affect the production of essential proteins and enzymes (Kong et al., 2010; Zhang et al., 2011). In this case, the superior antifungal effect of α-chitin nanofibers compared with native chitin was associated to nanofibers larger surface area, and consequently higher affinity with fungal cells. Another mechanism is based on the electrostatic interaction between the positively charged amino groups of the biopolymer and the negatively charged fungi cell surface, which can lead to the disruption of the cell wall (Muzzarelli et al., 2001).

Table 1
Colony forming units (CFU mL^{-1}) of α-chitin (CH) and chitin α-nanofibers (CHNF) with the respective fungal growth inhibition (FGI %) of CHNF on the growth of *A. niger*.

Sample	CFU (mL^{-1})	FGI (%)
CH	12,472	–
CHNF	1625	86.97

In this case, the superior antifungal activity of α-chitin nanofibers was due to the increased availability of amino groups because of their large surface area, leading to an increased electrostatic binding of the chitin nanofibers to anionic compounds at the fungi cell surface.

In future work comprehensive knowledge on antimicrobial activity and mode of action of chitin nanofibers will be done using other microorganisms and different environmental factors.

4. Conclusion

A straightforward and environmentally friendly concept to process α-chitin nanofibers was presented. α-Chitin nanofibers were successfully prepared from yellow lobster wastes with uniform width (bellow 100 nm) and high aspect ratio using dynamic high pressure homogenization. Moreover, there were no important changes in the chemical and crystal structure of α-chitin nanofibers compared to native α-chitin after the treatment. However, the conversion of native α-chitin to α-chitin nanofibers led to decrease in thermal degradation (around 50 °C).

The antifungal assays showed that the nano nature (small and compact size and high surface area/charge) of α-chitin nanofibers played an important role in the antifungal activity against *A. niger*. α-Chitin nanofibers presented a fungal growth inhibition (FGI) of 87%.

The resulting α-chitin nanofibers are very attractive not only as reinforcing fillers for nanocomposites applications but also for biomedical, food and textile industries, because of the many advantages compared to native chitin, including superior antifungal activity against *A. niger*.

Acknowledgments

The authors thankful for the financial support from the European Commission through the project ECLIPSE CP 280786 and the Department of Education, Universities and Investigation of the Basque Government through project IT672-13. The authors also acknowledge the technical and human support of General Research Services (SGIker) from the UPV/EHU for X-ray and ^{13}C NMR analysis.

References

Agulló, E., Mato, R., Peniche, C., Tapia, C., Heras, A., San Roman, J., et al. (2004). Quitina y Quitosano: Obtención, caracterización y aplicaciones. In A. Pastor de Abram (Ed.), *Fuentes y Procesos de Obtención* Perú, (pp. 105–154).

Brugnerotto, J., Lizardi, J., Goycoolea, F. M., Argüelles, W., Desbrieres, J., & Rinaudo, M. (2001). An infrared investigation in relation with chitin and chitosan characterization. *Polymer*, *42*, 3569–3580.

Chen, P., Lin, A. Y., Mckittrick, J., & Meyers, M. A. (2008). Structure and mechanical properties of crab exoskeletons. *Acta Biomaterialia*, *4*, 587–596.

Duarte, M. L., Ferreira, M. C., Marvão, M. R., & Rocha, J. (2002). An optimized method to determine the degree of acetylation of chitin and chitosan by FTIR spectroscopy. *International Journal of Biological Macromolecules*, *31*, 1–8.

Fan, Y., Fukuzumi, H., Saito, T., & Isogai, A. (2012). Comparative characterization of aqueous dispersions and cast films of different chitin nanowhiskers/nanofibers. *International Journal of Biological Macromolecules*, *50*, 69–76.

Fan, Y., Saito, T., & Isogai, A. (2008). Preparation of chitin nanofibers from squid pen β-chitin by simple mechanical treatment under acid conditions. *Biomacromolecules*, *9*, 1919–1923.

Fan, Y., Saito, T., & Isogai, A. (2010). Individual chitin nano-whiskers prepared from partially deacetylated α-chitin by fibril surface cationization. *Carbohydrate Polymers*, *79*, 1046–1051.

Feng, F., Liu, Y., & Hu, K. (2004). Influence of alkali-freezing treatment on the solid state structure of chitin. *Carbohydrate Research*, *339*, 2321–2324.

Focher, B., Beltranme, P. L., Naggi, A., & Torri, G. (1990). Alkaline N-deacetylation of chitin enhanced by flash treatments: Reaction kinetics and structure modifications. *Carbohydrate Polymers*, *12*, 405–418.

Goodrich, J. D., & Winter, W. T. (2007). α-Chitin nanocrystals prepared from shrimp shells and their specific surface area measurement. *Biomacromolecules*, *8*, 252–257.

Ifuku, S., Ikuta, A., Hosomi, T., Kanaya, S., Shervani, Z., Morimoto, M., et al. (2012). Preparation of polysilsesquioxane-urethaneacrylate copolymer film reinforced with chitin nanofibers. *Carbohydrate Polymers*, *89*, 865–869.

Ifuku, S., Nogi, M., Abe, K., Yoshioka, M., Morimoto, M., Saimoto, H., et al. (2009). Preparation of chitin nanofibers with a uniform width as α-chitin from crab shells. *Biomacromolecules*, *10*, 1584–1588.

Ifuku, S., Nogi, M., Abe, K., Yoshioka, M., Morimoto, M., Saimoto, H., et al. (2011). Simple preparation method of chitin nanofibers with a uniform width of 10–20 nm from prawn shell under neutral conditions. *Carbohydrate Polymers*, *84*, 762–764.

Ifuku, S., Nogi, M., Yoshioka, M., Morimoto, M., Yano, H., & Saimoto, H. (2010). Fibrillation of dried chitin into 10–20 nm nanofibers by a simple grinding method under acidic conditions. *Carbohydrate Polymers*, *81*, 134–139.

Jang, M.-K., Kong, B.-G., Jeong, Y.-I., Lee, C. H., & Nah, J.-W. (2004). Physicochemical characterization of α-chitin, β-chitin, and γ-chitin separated from natural resource. *Journal of Polymer Science Part A: Polymer Chemistry*, *42*, 3423–3432.

Kadokawa, J., Takegawa, A., Minea, S., & Prasad, K. (2011). Preparation of chitin nanowhiskers using an ionic liquid and their composite materials with poly(vinyl alcohol). *Carbohydrate Polymers*, *84*, 1408–1412.

Kong, M., Chen, X. G., Xing, K., & Park, H. J. (2010). Antimicrobial properties of chitosan and mode of action: A state of the art review. *International Journal of Food Microbiology*, *144*, 51–63.

Krajewska, B., Kyzioł, A., & Wydro, P. (2013). Chitosan as a subphase disturbant of membrane lipid monolayers. The effect of temperature at varying pH: II. DPPC and cholesterol. *Colloids and Surfaces A: Physicochemical and Engineering Aspects*, *434*, 359–364.

Krajewska, B., Wydro, P., & Jańczyk, A. (2011). Probing the modes of antibacterial activity of chitosan. Effects of pH and molecular weight on chitosan interactions with membrane lipids in Langmuir films. *Biomacromolecules*, *12*, 4144–4152.

Krajewska, B., Wydro, P., & Kyzioł, A. (2013). Chitosan as a subphase disturbant of membrane lipid monolayers. The effect of temperature at varying pH: I. DPPG. *Colloids and Surfaces A: Physicochemical and Engineering Aspects*, *434*, 349–358.

Kumirska, J., Czerwicka, M., Kaczyński, Z., Bychowska, A., Brzozowski, K., Thöming, J., et al. (2010). Application of spectroscopic methods for structural analysis of chitin and chitosan. *Marine Drugs*, *8*, 1567–1636.

Mincea, M., Negrulescu, A., & Ostafe, V. (2012). Preparation, modification, and applications of chitin nanowhiskers: A review. *Reviews on Advanced Materials Science*, *30*, 225–242.

Morin, A., & Dufresne, A. (2002). Nanocomposites of chitin whiskers from *Riftia* tubes and poly(caprolactone). *Macromolecules*, *35*, 2190–2199.

Muzzarelli, R. A. A., Muzzarelli, C., Tarsi, R., Miliani, M., Gabbanelli, F., & Cartolari, M. (2001). Fungistatic activity of modified chitosans against *Saprolegnia parasitica*. *Biomacromolecules*, *2*, 165–169.

Muzzarelli, R. A. A., Morganti, P., Morganti, G., Palombo, P., Palombo, M., Biagini, G., et al. (2007). Chitin nanofibrils/chitosan composites as wound medicaments. *Carbohydrate Polymers*, *70*, 274–284.

Paillet, M., & Dufresne, A. (2001). Chitin whisker reinforced thermoplastic nanocomposites. *Macromolecules*, *34*, 6527–6530.

Pinto, R. J. B., Almeida, A., Fernandes, S. C. M., Freire, C. S. R., Silvestre, A. J. D., Neto, C. P., et al. (2013). Antifungal activity of transparent nanocomposite thin films of pullulan and silver against *Aspergillus niger*. *Colloids and Surfaces B: Biointerfaces*, *103*, 143–148.

Plascencia-Jatomea, M., Viniegra, G., Olayo, R., Castillo-Ortega, M. M., & Shirai, K. (2003). Effect of chitosan and temperature on spore germination of *Aspergillus niger*. *Macromolecular Bioscience*, *3*, 582–586.

Qi, Z.-D., Fan, Y., Saito, T., Fukuzumi, H., Tsutsumi, Y., & Isogai, A. (2013). Improvement of nanofibrillation efficiency of α-chitin in water by selecting acid used for surface cationisation. *RSC Advances*, *3*, 2613–2619.

Raabe, D., Sachs, C., & Romano, P. (2005). The crustacean exoskeleton as an example of a structurally and mechanically graded biological nanocomposite material. *Acta Materialia*, *53*, 4281–4292.

Rabea, E. I., Badawy, M. E. T., Stevens, C. V., Smagghe, G., & Steurbaut, W. (2003). Chitosan as antimicrobial agent: Applications and mode of action. *Biomacromolecules*, *4*, 1457–1465.

Revol, J.-F., & Marchessault, R. H. (1993). In vitro chiral nematic ordering of chitin crystallites. *International Journal Biology Macromolecules*, *15*, 329–335.

Rinaudo, M. (2006). Chitin and chitosan: Properties and applications. *Progress in Polymer Science*, *31*, 603–632.

Wang, B., Li, J., Zhang, J., Li, H., Chen, P., Gu, Q., et al. (2013). Thermo-mechanical properties of the composite made of poly(3-hydroxybutyrate-co-3-hydroxyvalerate) and acetylated chitin nanocrystals. *Carbohydrate Polymers*, *95*, 100–106.

Watthanaphanit, A., Supaphol, P., Tamura, H., Tokura, S., & Rujiravanit, R. (2008). Fabrication, structure, and properties of chitin whisker-reinforced alginate nanocomposite fibers. *Journal of Applied Polymer Science*, *110*, 890–899.

Zeng, J. B., He, Y. S., Li, S. L., & Wang, Y. Z. (2012). Chitin whiskers: An overview. *Biomacromolecules*, *13*, 1–11.

Zhang, H. Y., Li, R. P., & Liu, W. M. (2011). Effects of chitin and its derivative chitosan on postharvest decay of fruits: A review. *International Journal of Molecular Sciences*, *12*, 917–934.

Zhao, H.-P., Feng, X.-Q., & Gao, H. (2007). Ultrasonic technique for extracting nanofibers from nature materials. *Applied Physics Letters*, *90*, 073112.